



Article

Ultrasound-Assisted Extraction Optimization of Proanthocyanidins from Kiwi (*Actinidia chinensis*) Leaves and Evaluation of Its Antioxidant Activity

Ji-Min Lv¹, Mostafa Gouda^{1,2,*} , Yan-Yun Zhu¹, Xing-Qian Ye¹ and Jian-Chu Chen^{1,*}

- ¹ National-Local Joint Engineering Laboratory of Intelligent Food Technology and Equipment, Zhejiang Key Laboratory for Agro-Food Processing, Zhejiang Engineering Laboratory of Food Technology and Equipment, College of Biosystems Engineering and Food Science, Zhejiang University, Hangzhou 310058, China; lvjimin@zju.edu.cn (J.-M.L.); 11813043@zju.edu.cn (Y.-Y.Z.); psu@zju.edu.cn (X.-Q.Y.)
- ² Department of Nutrition & Food Science, National Research Centre, Dokki, Giza 12422, Egypt
- * Correspondence: mostafa-gouda@zju.edu.cn (M.G.); jc@zju.edu.cn (J.-C.C.)

Abstract: Using ultrasound (US) in proanthocyanidin (PA) extraction has become one of the important emerging technologies. It could be the next generation for studying the US mechnophore impact on the bioactive compound's functionality. The objective of this study was to demonstrate the potential of US treatment on PAs extracted from kiwifruit (*Actinidia chinensis*) leaves, and to provide a comprehensive chemical composition and bioactivity relationship of the purified kiwifruit leaves PAs (PKLPs). Several methods like single-factor experiments and response surface methodology (RSM) for the four affected factors on US extraction efficiency were constructed. HPLC-QTOF-MS/MS, cytotoxicity analysis, and antioxidant activity were also demonstrated. In the results, the modeling of PA affected factors showed that 40% US-amplitude, 30 mL/g dry weight (DW) solvent to solid ration (S/S), and 70 °C for 15 min were the optimum conditions for the extraction of PAs. Furthermore, PKLPs exhibited significant radical scavenging and cellular antioxidant activity ($p < 0.05$). In conclusion, this study's novelty comes from the broad prospects of using US in PKLP green extraction that could play an important role in maximizing this phytochemical functionality in drug discovery and food science fields.

Keywords: proanthocyanidins; ultrasound-assisted extraction; kiwifruit leaves; extraction optimization; HPLC-QTOF-MS/MS; antioxidant potential



Citation: Lv, J.-M.; Gouda, M.; Zhu, Y.-Y.; Ye, X.-Q.; Chen, J.-C. Ultrasound-Assisted Extraction Optimization of Proanthocyanidins from Kiwi (*Actinidia chinensis*) Leaves and Evaluation of Its Antioxidant Activity. *Antioxidants* **2021**, *10*, 1317. <https://doi.org/10.3390/antiox10081317>

Academic Editors:
Sara Jaramillo-Carmona, Rafael Guillén Bejarano and Sergio López

Received: 31 July 2021
Accepted: 18 August 2021
Published: 21 August 2021

Publisher's Note: MDPI stays neutral with regard to jurisdictional claims in published maps and institutional affiliations.



Copyright: © 2021 by the authors. Licensee MDPI, Basel, Switzerland. This article is an open access article distributed under the terms and conditions of the Creative Commons Attribution (CC BY) license (<https://creativecommons.org/licenses/by/4.0/>).

1. Introduction

Kiwi (*Actinidia chinensis*) leaves are natural sources that are considered as a byproduct of kiwi fruit production and that contain a very high amount of natural bioactive phytochemicals that are generally considered as natural, safe extracts [1,2]. For instance, it has a high amount of polyphenols 189.39–440.71 mg GAE/g DW [3] that have a high bioactivity for human health (e.g., antioxidant and anti-tumor), due to their functional groups like hydroxyl groups on its phenolic rings [4]. In particular, proanthocyanidins (PAs) are a class of polyphenols that are divided into different types based on the hydroxylation patterns of their monomeric flavan-3-ols units [5], in which PAs oligo- or polymers are produced as an end product of the flavonoid biosynthetic pathway [6]. These phytochemicals are considered as offense and defense molecules because of their antioxidant [7], anticancer [8], antidiabetic [9], and antimicrobial activities [8]. Zheng et al. [10] reported that PAs are considered as a key ingredient that helps in the novel functional foods industry. For instance, they can inhibit the α -amylase enzyme activity in the phenolic-starch complexes. As a result, this reduces the starch digestibility, which has significant benefits for the delivery of functional molecules in humans [11].

Newly developed technologies are currently used for the extraction and structural analysis of PAs [12]. Regarding the emerging technologies for PA extraction, US has a

significant impact on increasing the efficiency of plant phytochemicals, especially polyphenolic PAs [13]. For example, using US for extraction of PAs from different plant origins like grape seeds and knotweed rhizome bark at 40 °C for 15–20 min enhanced their extracted yields [14,15]. Boulatov [16] reported that the mechanochemical effects of the US results in overstretching of macromolecule polymers (like carbohydrate and protein chains) that lead to their fragmentation and release of phytochemicals. A comparison study of US-assisted and conventional extraction methods on tea leaves' bioactive compounds showed that the breakdown of cells cytoarchitecture by US increased 20% of extracted bioactive phenolics [17]. In addition, Rashed et al. [18] reported that higher total phenolic content was extracted from *Lavandula pubescens* leaves using US compared to maceration extraction (ME).

For most plant leaves, the US acoustic cavitation can facilitate the flow of solvents into the plant cells and enhance the desorption of the bioactives from the matrix of solid samples. In addition, the formation of radicals during the optimum conditions of US process can increase the antioxidant activity of the extracted PAs through extension in the hydroxylation process [19]. This led to the fact that the optimum US conditions for various plant materials are maximizing the extracted yields and their bioactivities. In addition, US inhibits the hydrolyzing enzymes (e.g., α -glucosidase) that have a negative effect on flavonoids like PAs and their antioxidant functionality [20]. Collectively, the above information suggests a scope for optimization where maximum bioactivities could be obtained before the negative effects by heating or free radicals from the high US-amplitude. For instance, as a statistical technique, response surface methodology (RSM) has been proved as an effective tool for optimizing the process parameters that enable the reduction of the number of experimental trials and quantify the interactions between the multiple parameters [21]. Furthermore, several technologies, like high-performance liquid chromatography-Quadrupole Time of Flight Mass Spectrometry (HPLC-QTOF-MS/MS), and matrix-assisted laser desorption/ionization (MALDI), are recently validated as novel applicable methods for qualitative and quantitative analysis of PA structure conformation [12].

The use of bioactive PAs, as natural safe phytochemicals, in the prevention and treatment of different kinds of cancers has become one of the world's hottest scientific areas [22,23]. Nutraceuticals derived from fruits, vegetables, and herbal leaves (kiwi, pomegranate, orange) generally have multi-targeted anticancer potential with negligible side-effects, thus making them ideal candidates for non-pharmacologic anticancer therapies, especially for colorectal cancer (CRC), which remains the fourth most common cause of cancer-related deaths worldwide [24,25]. HepG-2 and Caco-2 cell lines that related to CRC are widely used to investigate the anticancer efficiency of the bioactive phytochemicals, especially PAs [26].

Therefore, this study aimed to evaluate the US impact on the extraction yield and chemical compositions of PAs extracted from kiwi leaves. Different US extraction conditions were evaluated to optimize the US conditions for PA extraction. Then, the optimum PA extract by using US was compared with its extract by ME for its anticancer and antioxidant functionality, thus providing evidence of the mechanochemical applicability of US as a green technology in the design of PA extraction while caring for their bioactive functionality. In addition, to evaluate the potential of using PAs as antioxidant and anticancer agents based on their unique chemical structures.

2. Materials and Methods

2.1. Chemicals and Materials

Acetone and ethanol that used in the part of extraction were purchased from Aladdin Reagent Co. Ltd. (Shanghai, China). AB-8 Macroporous resin was obtained from Solarbio Science and Technology Company (Beijing, China). Folin-Ciocalteu reagent was purchased from Aladdin Reagent Co., Ltd., Shanghai, China. Acetonitrile and formic acid of HPLC grade were purchased from Merck Chemicals (St. Louis, MO, USA). Deionized water was

used. Foetal bovine serum (FBS), Dulbecc's modified Eagle medium (DMEM), phosphate-buffered solution (PBS), penicillin/streptomycin (P/S), and methyl thiazolyl tetrazolium (MTT) were purchased from Life Technologies (Carlsbad, CA, USA).

Fresh Kiwi (*Actinidia chinensis*) leaves were collected during October from Zhuji local farm, Shaoxing, China. The cleaned leaves, as presented in Figure 1, were freeze-dried before being ground into powder and then pass through a 0.25 mm mesh screen. Kiwi leaves' powders were stored at $-20\text{ }^{\circ}\text{C}$ until further extraction.

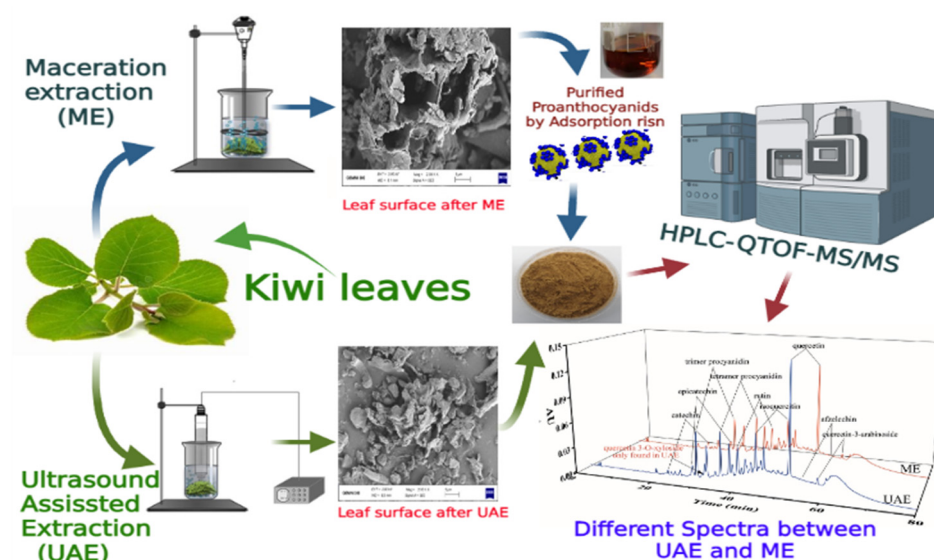


Figure 1. Flowchart of proanthocyanidins (PAs) extraction by ultrasound-assisted extraction (UAE) and Maceration extraction (ME) methods.

2.2. Extraction of PAs

2.2.1. Ultrasound-Assisted Extraction (UAE)

The ultrasound-assisted extraction technique was performed according to Martin-Garcia et al. [27]. In brief, 1 g of kiwi leaves' freeze-dried powders were mixed with an appropriate volume of acetone solvent (10–70 mL/g (S/S)) in 3.5 cm inner diameter cylindrical glass. UAE protocol was conducted by using different sonication power (0–70% US-amplitude), temperature (0–30 $^{\circ}\text{C}$), and time of ultrasonic bath system (JY92-IIDN, Ningbo Scientz Biotechnology Co., Ningbo, China). In addition, acetone was used as an ideal solvent for PA extraction from plants [27]. The supernatant was filtered by syringe filters (nylon membrane, pore size 0.45 μm) and then freeze-dried to obtain the PA crude extracts. The crude extracts were stored at 4 $^{\circ}\text{C}$ for further analysis.

2.2.2. Maceration Extraction (ME)

In order to compare the PAs extraction efficiency of UAE with the conventional methods, ME was carried out as described by Xu et al. [28] with slight modifications. An aliquot of 10 g of freeze-dried powder was mixed with 300 mL acetone solution (70%, *v/v*) at 30 $^{\circ}\text{C}$ and stirring at 200 rpm for 1 h. The extracted solution was filtered, freeze-dried, and stored at 4 $^{\circ}\text{C}$ in the same way as UAE.

2.3. Purification of the Extracted PAs

Crude extracts obtained in both UAE and ME were purified following Luo et al. [29]. In brief, the crude extracts (1 g) were loaded onto AB-8 Macroporous resin column and washed with distilled water (4 times column volume) to remove impurities, such as sugar, proteins, and pigments. Subsequently, 4 times column volume of ethanol solution (70%, *v/v*) was used to elute the PAs and the fraction filtered. Then, the extracts were lyophilized to remove the solvent and to obtain the PKLPs. Figure 1 presents the flowchart

of proanthocyanidin extraction by ultrasound-assisted extraction (UAE) and Maceration extraction (ME) methods. PA yield (%) was calculated by the following equation:

$$\text{PAs yield (\%)} = \frac{\text{dry weight of purified proanthocyanidins powders}}{\text{dry weight of kiwifruit leaves powders}} \quad (1)$$

2.4. Experimental Design

2.4.1. Single-Factor Experiments

Single-factor experiments were employed to determine the factors resulting in response values that were very close to the optimum region [30]. The response variable (Y) of extracted PAs was influenced by each independent parameter. In this part, the initial range of four designed factors were investigated including US amplitude (0–60%), sonication time (0–25 min), temperature (10–70 °C), and solvent to solid (S/S) ratio (10:1–70:1 mL/g).

2.4.2. Response Surface Methodology (RSM) Experiments

Based on the single-factor experimental results, the RSM was used to optimize the extraction of PAs, and its purpose was to explore the optimum condition to maximize the extraction efficiency of PAs. A central composite design (CCD) with four-factor and five-level was conducted for the best model due to its accurate prediction and economic approach [30,31]. In that model, US amplitude (X_1 , %), sonication time (X_2 , min), temperature (X_3 , °C), and solvent to solid ratio (X_4 , mL/g) were the independent variables, and their coded and uncoded levels were displayed in Table 1. Additionally, 30 experimental runs and 6 replicates of the center point were used to optimum the extraction model. In addition, the relationship between the four independent variables and the extraction yield of PAs was expressed as a second-order polynomial equation:

$$Y = \alpha_0 + \sum_{i=1}^n \alpha_i X_i + \sum_{i=1}^n \alpha_{ii} X_i^2 + \sum_{i=1}^n \sum_{j=1}^n \alpha_{ij} X_i X_j \quad (2)$$

where Y is the predicted value of extraction yield of PAs, α_0 is a constant; α_i , α_{ii} , and α_{ij} are the linear, quadratic, and interactive regression coefficients of the model, respectively; X_i and X_j are the independent variables.

Table 1. Response surface design with experimental and predicted results.

| Run | Factor X1 Amplitude % (Code) | Factor X2 Time Min (Code) | Factor X3 Solvent/Solid mL/g (Code) | Factor X4 Temp. °C (Code) | PAs (mg PC/g DW) | | TPC (mg CAT/g DW) | |
|-----|------------------------------------|---------------------------------|---|---------------------------------|------------------|-----------|-------------------|-----------|
| | | | | | Experimental | Predicted | Experimental | Predicted |
| 1 | 30 (−1) | 10 (−1) | 40 (+1) | 60 (+1) | 109.36 ± 7.23 | 105.81 | 162.11 ± 6.01 | 161.50 |
| 2 | 40 (0) | 15 (0) | 30 (0) | 50 (0) | 87.32 ± 5.15 | 85.01 | 135.69 ± 5.67 | 132.36 |
| 3 | 30 (−1) | 10 (−1) | 20 (−1) | 60 (+1) | 87.54 ± 4.87 | 84.45 | 131.92 ± 4.17 | 132.14 |
| 4 | 40 (0) | 5 (−2) | 30 (0) | 50 (0) | 80.65 ± 5.1 | 77.69 | 125.18 ± 3.69 | 123.71 |
| 5 | 40 (0) | 15 (0) | 30 (0) | 70 (+2) | 122.19 ± 5.71 | 119.55 | 177.15 ± 7.79 | 176.86 |
| 6 | 40 (0) | 15 (0) | 30 (0) | 50 (0) | 89.54 ± 3.57 | 85.01 | 127.91 ± 3.89 | 132.36 |
| 7 | 40 (0) | 25 (+2) | 30 (0) | 50 (0) | 94.18 ± 3.48 | 92.13 | 141.44 ± 7.70 | 144.40 |
| 8 | 40 (0) | 15 (0) | 50 (+2) | 50 (0) | 103.89 ± 4.18 | 99.67 | 141.37 ± 4.07 | 140.83 |
| 9 | 50 (+1) | 10 (−1) | 20 (−1) | 60 (+1) | 90.19 ± 5.08 | 86.29 | 133.61 ± 3.79 | 132.22 |
| 10 | 30 (−1) | 20 (+1) | 20 (−1) | 40 (−1) | 75.96 ± 3.52 | 71.63 | 120.24 ± 3.34 | 117.37 |
| 11 | 50 (+1) | 20 (+1) | 20 (−1) | 40 (−1) | 82.87 ± 4.11 | 81.07 | 138.44 ± 4.74 | 137.29 |
| 12 | 20 (−2) | 15 (0) | 30 (0) | 50 (0) | 81.73 ± 4.57 | 82.57 | 129.46 ± 4.77 | 132.58 |
| 13 | 50 (+1) | 10 (−1) | 40 (+1) | 60 (+1) | 105.18 ± 5.67 | 102.85 | 159.67 ± 3.93 | 158.42 |
| 14 | 40 (0) | 15 (0) | 30 (0) | 50 (0) | 86.99 ± 4.25 | 85.01 | 137.67 ± 5.15 | 132.36 |
| 15 | 50 (+1) | 10 (−1) | 20 (−1) | 40 (−1) | 74.68 ± 3.81 | 74.95 | 117.81 ± 2.95 | 115.55 |
| 16 | 50 (+1) | 20 (+1) | 40 (+1) | 60 (+1) | 116.42 ± 6.23 | 113.57 | 169.71 ± 5.41 | 168.57 |
| 17 | 50 (+1) | 10 (−1) | 40 (+1) | 40 (−1) | 83.67 ± 4.52 | 80.31 | 124.36 ± 3.72 | 128.91 |
| 18 | 30 (−1) | 20 (+1) | 40 (+1) | 40 (−1) | 84.08 ± 4.61 | 82.79 | 125.28 ± 3.35 | 124.91 |
| 19 | 30 (−1) | 20 (+1) | 40 (+1) | 60 (+1) | 121.11 ± 3.08 | 114.13 | 162.37 ± 5.73 | 160.45 |

Table 1. Cont.

| Run | Factor X1 Amplitude % (Code) | Factor X2 Time Min (Code) | Factor X3 Solvent/Solid mL/g (Code) | Factor X4 Temp. °C (Code) | PAs (mg PC/g DW) | | TPC (mg CAT/g DW) | |
|-----|------------------------------------|---------------------------------|---|---------------------------------|------------------|-----------|-------------------|-----------|
| | | | | | Experimental | Predicted | Experimental | Predicted |
| 20 | 40 (0) | 15 (0) | 10 (−2) | 50 (0) | 72.82 ± 4.06 | 71.95 | 105.06 ± 4.13 | 107.09 |
| 21 | 30 (−1) | 20 (+1) | 20 (−1) | 60 (+1) | 93.75 ± 4.35 | 91.77 | 145.66 ± 3.94 | 139.71 |
| 22 | 40 (0) | 15 (0) | 30 (0) | 50 (0) | 86.12 ± 3.56 | 85.01 | 137.27 ± 2.52 | 132.36 |
| 23 | 30 (−1) | 10 (−1) | 20 (−1) | 40 (−1) | 70.59 ± 4.11 | 67.91 | 107.45 ± 4.58 | 106.83 |
| 24 | 30 (−1) | 10 (−1) | 40 (+1) | 40 (−1) | 80.45 ± 4.19 | 78.07 | 127.30 ± 4.18 | 122.99 |
| 25 | 40 (0) | 15 (0) | 30 (0) | 50 (0) | 88.23 ± 5.07 | 85.01 | 127.13 ± 4.32 | 132.36 |
| 26 | 60 (+2) | 15 (0) | 30 (0) | 50 (0) | 95.19 ± 4.23 | 89.05 | 150.96 ± 4.48 | 149.42 |
| 27 | 40 (0) | 15 (0) | 30 (0) | 50 (0) | 88.37 ± 5.15 | 85.01 | 132.66 ± 3.95 | 132.36 |
| 28 | 40 (0) | 15 (0) | 30 (0) | 30 (−2) | 79.37 ± 4.51 | 76.87 | 122.94 ± 4.17 | 124.65 |
| 29 | 50 (+1) | 20 (+1) | 40 (+1) | 40 (−1) | 90.87 ± 4.81 | 87.43 | 146.06 ± 2.99 | 141.67 |
| 30 | 50 (+1) | 20 (+1) | 20 (−1) | 60 (+1) | 100.07 ± 6.28 | 96.01 | 150.82 ± 3.16 | 150.99 |

3D surface plots were constructed to exhibit the interactive effects between independent factors, which enabled the visualization of the relationships between the variables in the plot and the response.

2.5. Experimental Methods

2.5.1. Determination of Total Phenolics Content (TPC) and PAs Content and In Vitro Antioxidant Activity

Total phenolics were determined spectrophotometrically by using the Folin–Ciocalteu method following Gouda et al. [32] with minor modifications. The TPC of the extracts was expressed as mg of catechin (CAT) equivalents per g of sample.

The PA content was measured using the vanillin method described by Cao et al. [13]. Briefly, 0.5 mL of sample was mixed with 2.5 mL vanillin (1% in methanol, *v/v*) followed by 2.5 mL of H₂SO₄ (20% in methanol, *v/v*). The absorbance was measured at 500 nm after incubation at 30 °C for 20 min. Results were expressed on a dry weight basis (DW) as mg procyanidin (PC) equivalent per g of sample.

Diphenyl-1-picrylhydrazyl (DPPH) radical-scavenging activity and antioxidant power (ABTS) assays were employed to evaluate the antioxidant activity [1]. In brief, freeze-dried PKLPs were dissolved in phosphate buffer solution (PBS), and then 20 µL of the PKLPs (0–0.05 mg/mL) was mixed with 200 µL of methanolic solution of DPPH (0.04 mg/mL) and left for 30 min in the dark. The absorbance (Abs) was measured at the 517 nm wavelength using the EPOCH2 microplate reader (BioTek, Inc., Winooski, VT, USA).

The IC₅₀ values were calculated by using a regression equation between the concentration and the antioxidant percentage of each sample.

The antiradical power was measured using the 2,2′-azino-bis-3-ethylbenzothiazoline-6-sulphonic acid (ABTS) radical scavenging modified method of Gouda et al. [32]. Briefly, the ABTS stock solution (7 mM) was mixed with an equal volume of potassium persulfate (2.45 mM), then incubated at 4 °C for 16 h to produce ABTS radical cation (ABTS^{•+}). The ABTS^{•+} solution was diluted with distilled water to maintain an absorbance of 0.70 ± 0.01 at 734 nm. Then, 20 µL of 0–0.05 mg/mL PKLPs in PBS was mixed with 3 mL of ABTS^{•+} solution and kept in a dark place for 6 min at 25 °C before the measurement. The Abs was measured at 734 nm wavelength using an EPOCH2 microplate reader (BioTek, Inc., Winooski, VT, USA). IC₅₀ was measured using the same formula of the DPPH method. All of the measurements were performed in three replicates.

2.5.2. HPLC-QTOF-MS/MS Analysis

Separation and structure identification of PKLPs was conducted using a reversed-phase HPLC system (Waters e2695, Waters Corp., Milford, MA, USA) following the method of Huang et al. [33] with minor modifications. The system included a quaternary pump coupled UV-Vis detector (Waters 2489, Waters Corp., Milford, MA, USA) and equipped

with Agilent Zorbax Extend-C18 column (4.6 × 250 mm, 5 μm, (Agilent Tech Co., City, CA, USA). In brief, the injected volume was 10 μL, 35 °C with the flow rate of the mobile phase fixed at 0.7 mL/min, and the detection wavelength was set at 280 nm to monitor all phenolic compounds. Two elution solvents, A (water: formic acid; 99.7: 0.3, *v/v*) and B (acetonitrile), were used with the following gradient elution program: 3% B (0 min); 3–25% B (0–56 min); 24–67% B (56–79 min); 100% B (79–80 min).

MS spectra were recorded on a Triple-TOF 5600+ ion trap mass spectrometer (AB scientific, Framingham, MA, USA). The mass spectrometer was operated in negative ion mode using the following conditions: 50–1500 *m/z* mass range, 10 V capillary voltage, 550 °C capillary temperature, 4.5 kV ion spray voltage, 35 arb sheath gas (N₂), 6 arb auxiliary gas (N₂), and 80 V tube lens offset voltage.

2.5.3. Cell Culture and Treatment

Caco-2 (human colorectal adenocarcinoma) cell lines were provided by Zhejiang Key Laboratory for Agro-Food Processing (Zhejiang University, Hangzhou, China). The cells were cultured at 37 °C, in Dulbecco's modified eagle medium (DMEM) medium with 20% Fetal Bovine Serum (FBS) and 1% penicillin-streptomycin (P/S) under 5% CO₂. Cells were subcultured 3–4 times per week by replacing fresh medium to keep the cells in a good growth state.

2.5.4. Cytotoxicity Analysis

The cytotoxicity effect of extracted PAs on Caco-2 cells were tested following Gao et al. [34] with some modification. In addition, 100 μL of Caco-2 cells was seeded into 96-well plates at a density of 2 × 10⁵ cells/well and incubated for 48 h in standard cell culture condition before being replaced by fresh medium. Then, 10 μL of samples with various concentrations (0–125 μg/mL) were added to each well, and the control was treated without a sample solution; the blank wells only contain growth medium. After incubating for 24 h, 20 μL of MTT (0.5 mg/mL) was added, and the plates were incubated 4 h at 37 °C under 5% CO₂. Afterwards, the medium was removed, and 100 μL of DMSO was added to dissolve the MTT-formazan complex. The absorbance of the cells was measured at 570 nm and compared to the control. The IC₅₀ values were calculated after plotting cell viability versus reagent concentration.

2.5.5. Antioxidant Activity on H₂O₂-Induced Cell Death in Caco-2 Cells Injured Cell Model Induced by H₂O₂

The antioxidant activity on H₂O₂-induced cell death on Caco-2 cells was determined according to Cilla et al. [26]. Briefly, 5 mL medium contains 2 × 10⁶ cells/well was pipetted into 6-well plate (Costar Corning, Rochester, NY, USA), and incubated at 37 °C under 5% CO₂ for 24 h. Then, serial dilutions (0–250 μg/mL) of H₂O₂ multiple times (0–5 h) were added to each well to determine the IC₅₀ concentration of H₂O₂ in the injured Caco-2 cells, which aim to establish the H₂O₂-induced oxidative injury model. The results were expressed as cell viability measured by the MTT assay.

Intracellular Antioxidant Activity Assay

The effect of extracted PAs' antioxidant activity on the Caco-2 cells was measured according to Liang et al. [35]. Briefly, 5 mL medium containing 2 × 10⁵ cells/well was pipetted into 96-well plates. The medium was replaced with a fresh medium after cultivation for 24 h at 37 °C. The experimental group was treated with various concentrations of samples (0–125 μg/mL, 10 μL) for 24 h before H₂O₂ treatment, the control group was normally cultivated, and the model group was treated with H₂O₂. The result was expressed as the cell viability determined by the MTT assay.

2.6. Statistical Analysis

Experiments were conducted in triplicate and the average values \pm standard deviation (SD) are tabled. Data were further analyzed via one-way analysis of variance (ANOVA), using SPSS 19.0 (Chicago, IL, USA). Analysis of variance (ANOVA) and correlation efficient (r^2) were applied among all the measurements, $p \leq 0.05$ was considered statistically significant or correlated, and $p \leq 0.01$ was considered as highly significant. Tukey's HSD test and Least significant differences (LSD) have been calculated to measure the signification among the tested groups and properties. In addition, IC_{50} was calculated based on the regression equation.

3. Results

The optimization of the UAE method on the functionality of the extracted PAs from kiwi leaves is important for further studying their exact potential bioactivity. This is because US shows high potential in the field of herbal science due to its high ability to generate better yield and low scale-up finance compared to the other emerging techniques like a microwave (MW) and pulsed electric fields (PEF) [36]. On the other hand, special attention should be focused on the chemical composition and bioactivity of extracted PAs [4]. Thus, this study conducted a single-factor experimental design to show the optimum of four significant US factors represented in power, duration, temperature, and solvent to solid ratio that have significant influences on PA extraction.

3.1. Single-Factor Experimental Analysis

Single-factor experiments were designed to evaluate the influences of the four US-related factors (amplitude, sonication time, extraction temperature, and S/S ratio) on PA extraction yields (Figure 2). These experiments presented four different factors that could affect the extraction efficiency of PAs from kiwi leaves.

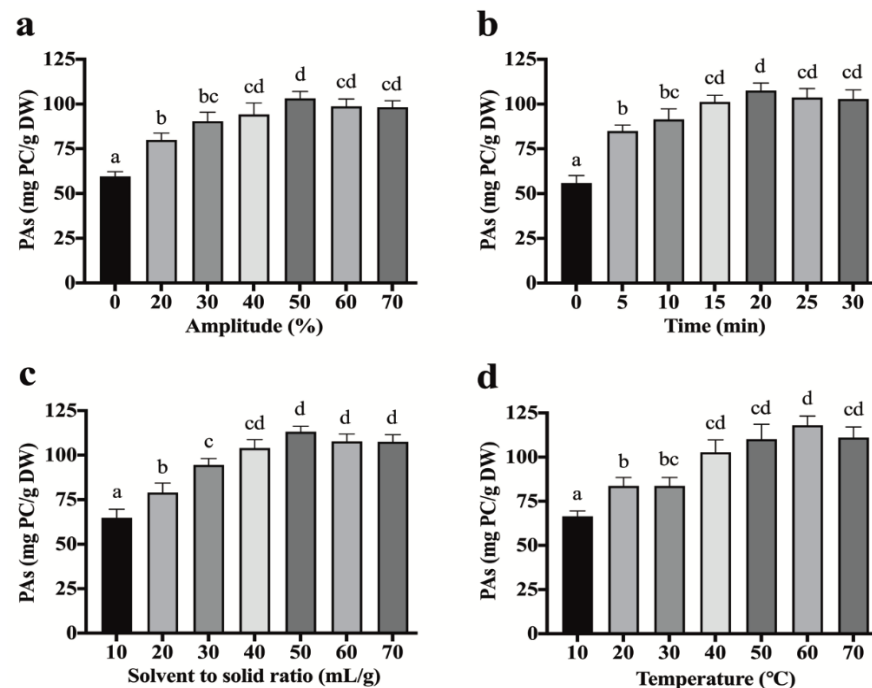


Figure 2. Single factor experiments of the UAE parameters' effects on yield of PAs extracted from kiwifruit leaves: (a) ultrasonic amplitude; (b) extraction time; (c) solvent to solid ratio; and (d) extraction temperature. Mean \pm SD with different alphabet superscript within the same column and analytical parameter indicate that values differ significantly ($p < 0.05$).

3.2. Effect of US Amplitude on PA Extraction

In order to improve the US-assisted efficiency of extracted PAs from kiwifruit leaves, ultrasonic amplitude (0, 20, 30, 40, 50, 60, 70%) was carried out. Other parameters were at fixed conditions (15 min, 30 °C, and 30 mL/g S/S ratio). A significant ($p < 0.05$) increase in PA yield (79.90 ± 3.91 mg PC/g DW) after 15 min, and the highest extracted yield was obtained at 50% (103.12 ± 3.93 mg PC/g DW) compared to the control with 59.58 ± 2.67 mg PC/g DW (Figure 2a). Then, reverse effects have happened from 60% (98.69 ± 4.09 mg PC/g DW), but the differences did not attend the significant level ($p > 0.1$). This phenomenon could be explained by the potential increase in the cavitation bubbles by an increase in ultrasonic power, which increases the solvent intracellular transfer. A US mechanophore breakage (mechanochemical breakage of the polymer reactive units like cyclic rings) can occur in extracts' solutions via the shear stress caused by the collapse of US-induced cavitation bubbles [37,38]. These modifications in the structure of extracted compounds caused by US can facilitate the bioavailability of the bioactive molecules extracted from plants [16]. However, the US higher than 50% had a negative effect on the PAs due to the formed radicals and H_2O_2 by the cavitation's bubbles [4]. Therefore, 50% amplitude was selected as the optimum used power for the extraction of PAs. Zhao et al. [39] reported that high US-amplitude (600 W) significantly degraded the extracted phytochemicals.

3.3. Effect of Sonication Time on PAs

To optimize the extraction capacity of UAE for the recovery of PAs, various ranges of sonication time (0, 5, 10, 15, 20, 25, 30 min) were evaluated. Other parameters were fixed at 30% US amplitude, 30 °C temp., and 30 mL/g S/S ratio. It has been observed that the yield of PAs was increased significantly ($p < 0.05$) with sonication time of up to 20 min (107.51 ± 4.28 mg PC/g DW) compared to the control with 55.82 ± 4.32 mg PC/g DW. Then, a slight decrease happened in a longer duration (25, 30 min). Patil and Akamanchi [40] used US (20 kHz, 150 W, 30 °C) for extraction of camptothecin from *Nothapodyhtes nimmoniana* leaves. They mentioned that the application of US increased the camptothecin yield (1.7-fold) and decreased the extraction time from 6 h to 18 min. This could be due to the potential impact of US to transform the disulfide bonds to thiol bonds of the molecules, which results in changing the covalently attached linear polymer chains in the β -position to a disulfide moiety [41]. However, long-time ultrasonic cavitation could result in the degradation of polyphenolics that declined the extraction yield [4]. Therefore, 20 min was selected as a suitable US time range for PAs.

3.4. Effect of Sonication Temperature on PAs

The effect of extraction temperature on PAs was performed from 10–70 °C with other fixed parameters (30% ultrasonic amplitude, 15 min sonication time, and 30 mL/g S/S ratio). The experimental results showed that, by raising the temperature of extraction from 10 to 60 °C, the yield of PAs was significantly increased from 66.48 ± 3.06 to 118.03 ± 5.20 mg PC/g DW. Then, the PA yield decreased upon further increasing of the temperature (Figure 2d). Additionally, the effect was similar to the increase in US-amplitude and time. These results might be related to the decrease of surface tension and viscosity of the solvent, which induced an increase in vapor pressure. With the increment of temperature, the sonochemical influents caused by the collapse of cavitation bubbles decreased, and polyphenols might be degraded at a higher temperature situation [4]. Therefore, controlling the temperature at an appropriate range is very necessary during the extraction process of bioactive compounds from plant materials, for which the extracted PAs by US can show a higher antioxidant capacity against DPPH, and hydroxyl radicals compared to heat reflux extraction based on the significant differences in the extracted chemical structure [42]. In addition, Huo et al. [41] reported that US mechanochemistry could decrease the exposure temperature at the molecular level by rearranging or cleaving bonds at predetermined breaking sites that could assist in facilitating the release of PAs in the lower temperature compared to the maceration method [43].

3.5. Effect of Solvent to Solid Ratio during the Sonication Process on PAs

To maximize the extraction efficiencies, various S/S ratios (10, 20, 30, 40, 50, 60, 70 mL/g) were selected with other fixed parameters (30% US amplitude, 15 min, and 30 °C). As presented in Figure 2c, the yield of PAs increased significantly ($p < 0.05$) at 50 mL/g (113.03 ± 3.10 mg PC/g DW) compared to 10 mL/g with 64.88 ± 4.83 mg PC/g DW. After reaching a peak, the yield of PAs slightly decreased when the S/S ratio further increased above 50 mL/g. A possible explanation is that the US cavitation effect could decrease the concentration of the high S/S ratio level by improving the rates of heat and mass transfer, cell disruption, and the penetration of solvents to the herbal tissues [13,44]. Xu et al. [21] reported that 40 mL/g of S/S was the most efficient solvent concentration, which improved the solubility of PAs in the plant cells. Boulatov [16] reported that the US mechanochemistry affected overstretching carbohydrates' polymers that lead to their fragmentation, which helps in releasing small molecules that are bound in their polymer chain.

3.6. Analysis of Response Surface Methodology

3.6.1. Model Fitting

The experimental data of extracted PAs from kiwi leaves ranged from 70.59 to 122.19 mg PC/g DW, and TPC ranged from 105 to 177.15 mg CAT/g DW (Table 1). They were optimized based on the CCD and evaluated by the linear regression and ANOVA (Table 2). In addition, the applicability of the model is typically dependent on the realization of the significant regression coefficient (R^2) and insignificant lack of fit [45,46]. The importance of measuring TPC with PAs was due to their strong correlations, as PAs belong to TPC [14], with the possibility of selecting the conditions with the highest concentration of TPC (177.15 mg CAT/g DW), and, as a consequence, stronger validation of PA extracts with 122.19 mg PC/g DW at the same condition of 40% (US-amplitude), 15 min, 30 mL/g (S/S ratio), and 70 °C (Table 1). Leontowicz et al. [47] mentioned the strong correlation between TPC and flavanols in kiwi fruit. This can indicate the suitability of the used extraction conditions of PAs, as flavan-3-ols, through its verification by total phenolic contents.

Table 2. Analysis of Variance (ANOVA), factors, and their interaction effects.

| Source | Sum of Squares | df | Mean Square | F-Value | p-Value |
|--------------------------------------|----------------|----|-------------|---------|---------|
| Model | 5213.5733 | 14 | 372.3981 | 89.90 | <0.0001 |
| X₁-Amplitude | 96.1200 | 1 | 96.1200 | 23.20 | 0.0002 |
| X₂-Extraction Time | 341.4867 | 1 | 341.4867 | 82.44 | <0.0001 |
| X₃-Solvent: solid | 1314.6840 | 1 | 1314.6840 | 317.38 | <0.0001 |
| X₄-Temperature | 2950.1620 | 1 | 2950.1620 | 712.20 | <0.0001 |
| X₁X₂ | 5.7002 | 1 | 5.7002 | 1.38 | 0.2591 |
| X₁X₃ | 22.1606 | 1 | 22.1606 | 5.35 | 0.0353 |
| X₁X₄ | 27.3268 | 1 | 27.3268 | 6.60 | 0.0214 |
| X₂X₃ | 1.0868 | 1 | 1.0868 | 0.26 | 0.6160 |
| X₂X₄ | 13.4873 | 1 | 13.4873 | 3.26 | 0.0913 |
| X₃X₄ | 129.6752 | 1 | 129.6752 | 31.30 | <0.0001 |
| X₁² | 1.6450 | 1 | 1.6450 | 0.40 | 0.5381 |
| X₂² | 0.0073 | 1 | 0.0073 | 0.00 | 0.9670 |
| X₃² | 1.3113 | 1 | 1.3113 | 0.32 | 0.5820 |
| X₄² | 303.2210 | 1 | 303.2210 | 73.20 | <0.0001 |
| Residual | 62.1349 | 15 | 4.1423 | | |
| Lack of Fit | 54.8974 | 10 | 5.4897 | 3.79 | 0.0771 |
| Pure Error | 7.2375 | 5 | 1.4475 | | |
| Cor Total | 5275.7082 | 29 | | | |
| R² | 0.9882 | | | | |
| Adjusted R² | 0.9772 | | | | |
| Predicted R² | 0.9381 | | | | |
| Adeq. Precision | 37.40 | | | | |
| Mean | 90.7793 | | | | |
| C.V. % | 2.2420 | | | | |

In this study, R^2 was highly significant ($R^2 = 0.9882$) and the lack of fit was insignificant (p -value = 0.0771), which indicates that the prediction model was valid for PA extraction. Meanwhile, there are adjusted and predicted coefficients ($R_{\text{adj}}^2 = 0.9772$ and $R_{\text{pre}}^2 = 0.9381$) and the high-value Adeq. precision (37.40) with a low value of the coefficient of variation (C.V. = 2.24%), which indicated a high reliability of experimental data with a very high degree of precision (Figure 3). Esua et al. [48] mentioned that C.V. values < 10% for responses suggesting the reliability, precision, and reproducibility of the established experiments. Therefore, the current analysis showed that both mathematical models for calibration and prediction were acceptable in describing the results of US-assisted extraction for kiwi leaves. In addition, this study experimental model agreed with Ismail et al. [49], who reported that the coefficient of variation (C.V. < 0.2445) indicates a low variation in the mean values and a higher degree of precision and reliability.

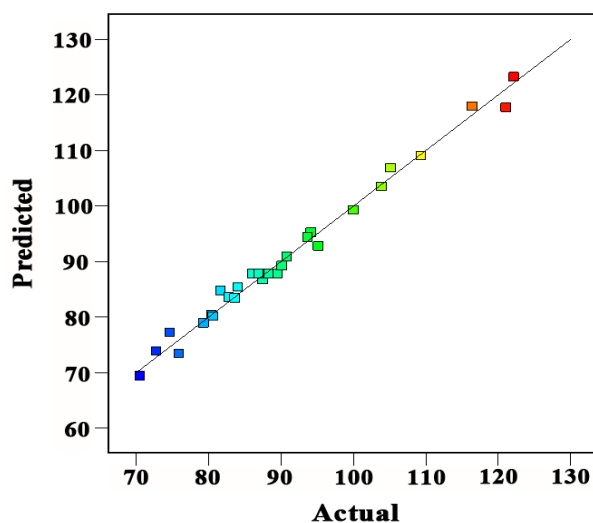


Figure 3. Correlation between the actual and predicted values of extracted yield of proanthocyanidins (PAs) from kiwifruit leaves.

3.6.2. Interaction of Independent Variables on Extraction PAs in the RSM Model

As presented in Table 2, the linear regression coefficients of US-amplitude (X_1); extraction time (X_2); S/S ratio (X_3); and extraction temperature (X_4) were significant ($p < 0.05$). However, X_1X_2 , X_2X_3 , X_2X_4 , X_1^2 , X_2^2 , and X_3^2 were insignificant ($p > 0.05$), which indicates a highly significant effect on the surface response [50]. According to experimental results, the final predictive second-order polynomial equation describes the effectiveness of extracted PAs by UAE, taking into consideration only the significant parameters, which was presented in the following equation:

$$Y = 105.39 + 0.83X_1 - 0.78X_2 - 0.42X_3 - 2.82X_4 - 0.01X_1X_3 - 0.01X_1X_4 + 0.03X_3X_4 + 0.03X_4^2 \quad (3)$$

where Y represents the yield of PAs; X_1 , X_2 , X_3 , and X_4 are the coded variables for the ultrasonic amplitude, ultrasonic time, S/S ratio, and extraction temperature, respectively.

3.6.3. Response Surface Methodology of the Four US Affected Factors' Variables

Three-dimensional response surface and contour plots (Figure 4) were used to illustrate the interactive effects between four independent variables and the extraction yield of PAs [51]. The PAs (z -axis) were plotted against two independent variables while keeping the rest of the variables at a fixed level. Figure 4a displayed the interactive effect between US-amplitude and time on the yield of PAs with the S/S ratio and extraction temperature at a fixed value. The yield of PAs was significantly increased with the exposure time, and it was slightly increased with increasing US-amplitude. The best explanation for this phenomenon is that temperature from the higher US-amplitude is increasing the mass

transfer, facilitating the release of molecules from the leaves' tissues [4]. An increase of S/S from 10 to 50 mL/g increased the extraction yield of PAs significantly, while the extraction yield of PAs increased slightly with the enhancement of ultrasonic amplitude from 20% to 60% (Figure 4b). On the other hand, the values of PAs increased dramatically with increasing the extraction temperature, reaching the optimum level at 50–70 °C (Figure 4c). The temperature had a significant effect on extraction while the influence of US-amplitude on the response did not attend a significant level ($p > 0.1$) since temperature had a dual effect on both solvent and solute. Guo et al. [52] mentioned that the adsorption ratio of the flavonoids was negatively correlated with the temperature. PAs as flavons are facilitating their release from leaves by increasing temperature. The PAs were shown in Figure 4d as the interactive influence on ultrasonic time and S/S ratio. PAs increased rapidly as the function of S/S ratio, while the ultrasonic time had a slight effect on the extraction of PAs. The highest values of PAs were observed at a longer extractive time and higher S/S ratio. Meanwhile, the maximum extraction of PAs could be obtained at a longer extractive time and higher temperature with other extraction parameters being fixed (Figure 4e). Ismail et al. [49] reported that US for 20 min and 30% US-amplitude was the optimum condition for PA yield. In that study, the higher amplitude during ultrasonic irradiation resulted in the oxidization of PAs, which caused the decline of extraction yield. Moreover, the interactive effect of S/S ratio and temperature demonstrated a significant interrelation between both influencing factors (Figure 4f). According to the response model, the PA yield increased with an increase in S/S ratio and temperature until 50 mL/g and 70 °C as the highest condition.

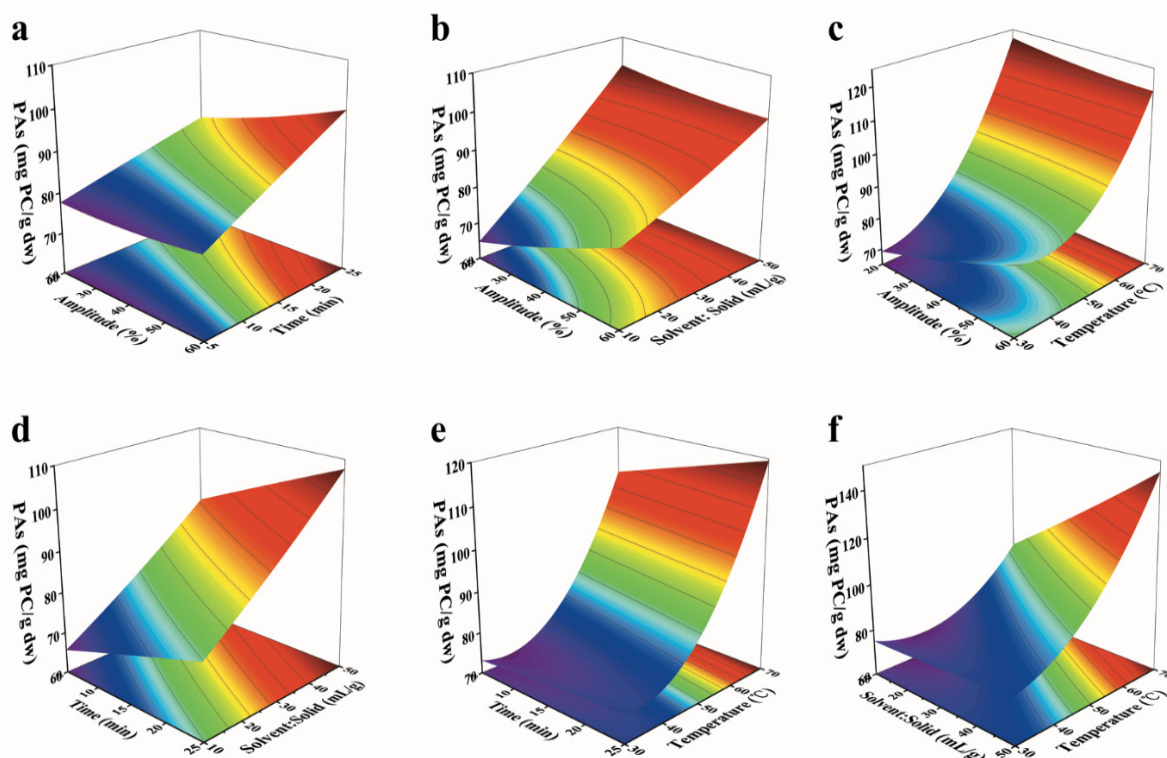


Figure 4. Response surface methodology (RSM) for the ultrasound-assisted extraction (UAE) of extracted yield of proanthocyanidins (PAs) from kiwi leaves with respect to ultrasonic amplitude (X1); extraction time (X2); solvent to solid ratio (X3); and extraction temperature (X4). (a) RSM between amplitude and time; (b) RSM between amplitude and solvent to solid ratio; (c) RSM between amplitude and temperature; (d) RSM between time and solvent to solid ratio; (e) RSM between time and temperature; (f) RSM between solvent to solid ratio and temperature.

The final optimum UAE conditions were concluded as follows: 40% (US-amplitude), 15 min, 30 mL/g (S/S ratio), and 70 °C. Meanwhile, the experimental yield of PAs was

close to the predicted yield (confidence level > 98%)—in which, under the optimal UAE conditions, PA experimental values were 122.19 mg PC/g DW, which was matched well with the predicted value (119.55 mg PC/g DW).

3.7. Comparison between Ultrasound-Assisted Extraction (UAE) and Traditional Maceration Extraction (ME) Efficiency and Identification of PA Fractions

In order to validate the effectiveness of ultrasound on the extraction of PAs from kiwi leaves, a comparison was carried out between UAE and ME. ME is considered a common technique that has been employed numerous times by different researchers for the extraction of polyphenol and PAs [27,53,54]. It was observed that UAE significantly increased the extracted PA yield ($11.3 \pm 1.41\%$) compared to the maceration method ($8.65 \pm 1.2\%$) for which ABTS and DPPH showed that the antioxidant activity of ultrasound-assisted extracts was significantly ($p < 0.05$) higher than ME (Table 3).

Table 3. Comparative yield, PAs, and chemical-based antioxidant activity of kiwifruit leaves by different extractions.

| Response | Yield (%) | PAs (mg PC/g DW) | ABTS IC ₅₀ (µg/mL) | DPPH IC ₅₀ (µg/mL) |
|----------|-------------------|---------------------|-------------------------------|-------------------------------|
| UAE | 11.3 ± 1.41^b | 122.19 ± 5.71^b | 10.88 ± 0.31^a | 13.67 ± 0.39^a |
| ME | 8.65 ± 1.20^a | 93.7 ± 5.69^a | 13.67 ± 0.39^b | 17.59 ± 0.44^b |

Mean \pm SD with different alphabet superscript within the same column and analytical parameter indicate that values differ significantly ($p < 0.05$).

Additionally, the fraction of phenolics by HPLC-QTOF-MS/MS showed a higher relative percentage of several sensitive compounds like benzoyl glucuronide, catechin, and isoquercetin in UAE compared to ME (Table 4; Table S1; Figure 5). Meanwhile, quercetin 3-O-xyloside was found in UAE, which means that the validation of the optimum condition in extracting PA compounds can enhance the efficiency of the separated phytochemicals.

Table 4. Extracted compositions identified by HPLC-QTOF-MS/MS.

| Time (min) | Formula | Mass (<i>m/z</i>) | Compound Identification | MS/MS Fragment (<i>m/z</i>) | UAE | ME |
|------------|---|---------------------|-----------------------------|-------------------------------|----------------------|--------|
| | | | | | Relative Percent (%) | |
| 18.36 | C ₂₀ H ₂₂ O ₅ | 341 | caffeyl glucopyranose | 326; 319; 253; 225 | 0.862 | 0.844 |
| 21.47 | C ₁₃ H ₁₄ O ₈ | 297 | benzoyl glucuronide | 179; 135; 297 | 1.749 | 0.903 |
| 22.33 | C ₃₀ H ₂₆ O ₁₃ | 593 | dimer propelargonidins | 441; 467; 425 | 0.822 | 0.597 |
| 23.31 | C ₂₁ H ₂₂ O ₁₂ | 465 | taxifolin hexoside | 285; 179; 301 | 0.461 | 0.343 |
| 24.72 | C ₁₅ H ₁₄ O ₆ | 289 | catechin | 289; 181; 137; 125; 151 | 2.137 | 1.048 |
| 27.91 | C ₃₀ H ₂₆ O ₁₂ | 577 | dimer procyanidin | 577; 449; 425; 289; 287 | 3.399 | 3.135 |
| 28.95 | C ₃₀ H ₂₆ O ₁₂ | 577 | dimer procyanidin isomer | 577; 449; 425; 289; 287 | 9.022 | 8.308 |
| 30.39 | C ₂₀ H ₁₈ O ₁₁ | 433 | quercetin 3-O-xyloside | 325; 300; 285; 151 | 0.485 | - |
| 31.54 | C ₁₅ H ₁₄ O ₆ | 289 | epicatechin | 289; 181; 137; 125; 151 | 6.77 | 5.68 |
| 35.01 | C ₄₅ H ₃₈ O ₁₈ | 865 | trimer procyanidin | 577; 451; 407; 289 | 7.483 | 7.62 |
| 37.24 | C ₆₀ H ₅₀ O ₂₄ | 1153 | tetramer procyanidin | 865; 577; 451; 289 | 5.949 | 6.044 |
| 39.24 | C ₆₀ H ₅₀ O ₂₄ | 1153 | tetramer procyanidin isomer | 865; 577; 451; 289 | 8.423 | 6.475 |
| 41.33 | C ₂₇ H ₃₀ O ₁₆ | 610 | rutin | 301 | 2.953 | 2.857 |
| 45.56 | C ₂₁ H ₂₀ O ₁₂ | 463 | isoquercetin | 301; 287; 151 | 6.112 | 4.001 |
| 51.51 | C ₂₁ H ₂₀ O ₁₁ | 447 | quercetin | 301; 271; 243; 179 | 18.617 | 17.782 |
| 54.74 | C ₁₅ H ₁₄ O ₅ | 273 | afzelechin | 273; 147; 138; 126 | 0.305 | 0.212 |
| 58.05 | C ₂₀ H ₁₈ O ₁₁ | 433 | quercetin-3-arabinoside | 300; 179 | 1.262 | 1.064 |

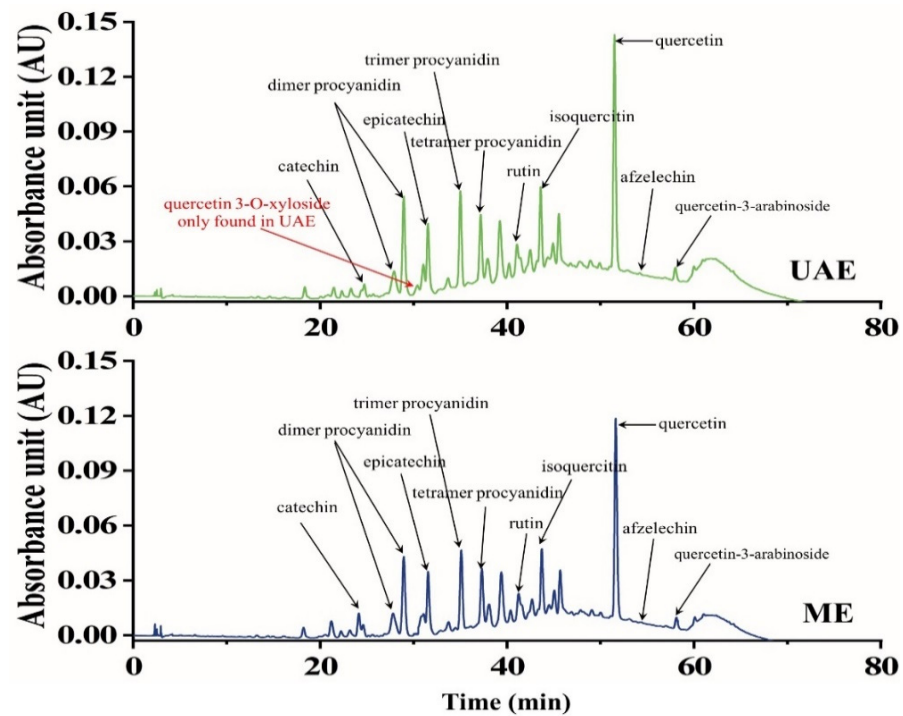


Figure 5. HPLC-QTOF-MS/MS spectra of the chemical composition differences between ultrasound-assisted extraction (UAE) and maceration extraction (ME) methods.

In addition, a scanning electron microscope showed high differences between using UAE and ME through an obvious degradation of leaves' fibers microstructure by US after 30 min and 60 min compared to maceration (Figure 6).

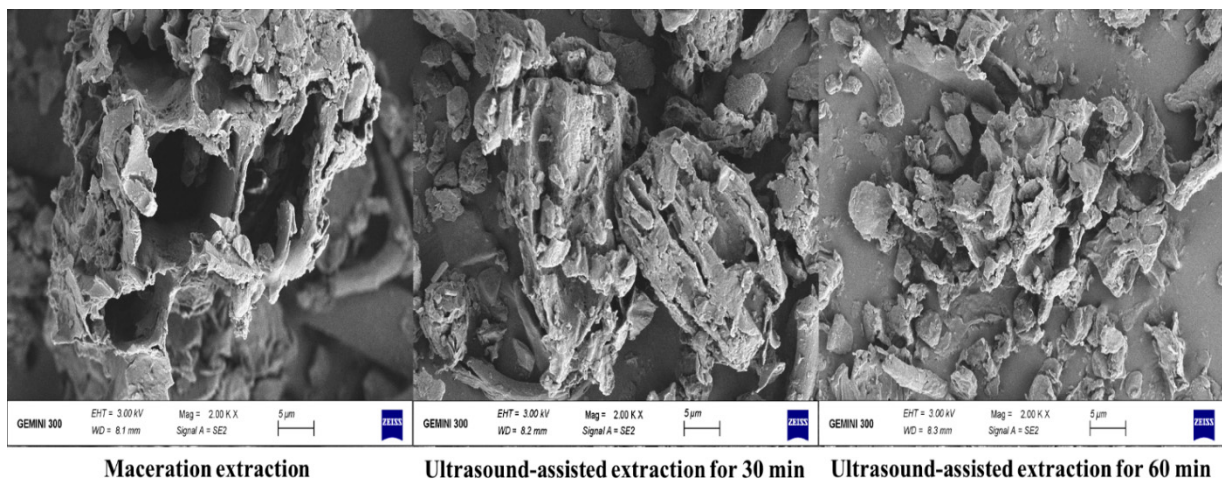


Figure 6. Scanning electron micrographs of ultrasound-assisted extraction (UAE) and Maceration extraction (ME) methods.

These differences in intramacromolecules' connective tissues facilitated the release of PAs in US-treated samples. Similar observations have been reported for US treatment by Esua, Cheng, and Sun [48]. In addition, Pudziulyte et al. [55] reported that US significantly increased the extracted phenolic yield (855.54 $\mu\text{g/g}$) of *Isholtzia ciliata* leaves compared to the maceration method (141.06 $\mu\text{g/g}$) through microstructure degradation. They mentioned that US for 11 min increased the mass fraction of total phenols by 20% compared to water bath shakers for 30 min with the same solvent.

3.8. Evaluation of Bioactive Functionality of the Extracted PAs by Cytotoxicity and Cellular Antioxidant Assays

Due to the global concern of cancer treatment by natural safe bioactive molecules [22], in this study, the extracted PAs' functionality has been evaluated. The cytotoxicity anticancer activity through seven concentrations (5, 10, 25, 50, 75, 100, 125 $\mu\text{g/mL}$) of PAs against HepG-2 and Caco-2 cell line revealed the high efficiency of the extracted PAs by optimized conditions of UAE. A marked reduction in the probable cancer risk was observed for the exposure against the two species (Figure 7), and there was a significant reduction ($p < 0.01$) in Caco-2 cell viability after 25 $\mu\text{g/mL}$ (Figure 7a). Meanwhile, the significant reduction ($p < 0.05$) in HepG-2 cell viability was after 50 $\mu\text{g/mL}$. Moreover, Caco-2 was more sensitive to PAs compared to HepG-2. Kumari and Gupta [51] reported a marked reduction in probable cancer under RSM optimized conditions. In addition, the mechanistic and preclinical studies demonstrated that the capacity of PAs to modulate the several factors related to colorectal cancer is based on its polymerization degree [56]. Leontowicz et al. [47] mentioned that high polyphenolic and flavonoids, flavanols, and tannins' contents of kiwi have a very significant inhibition impact on the growth of cancer cells.

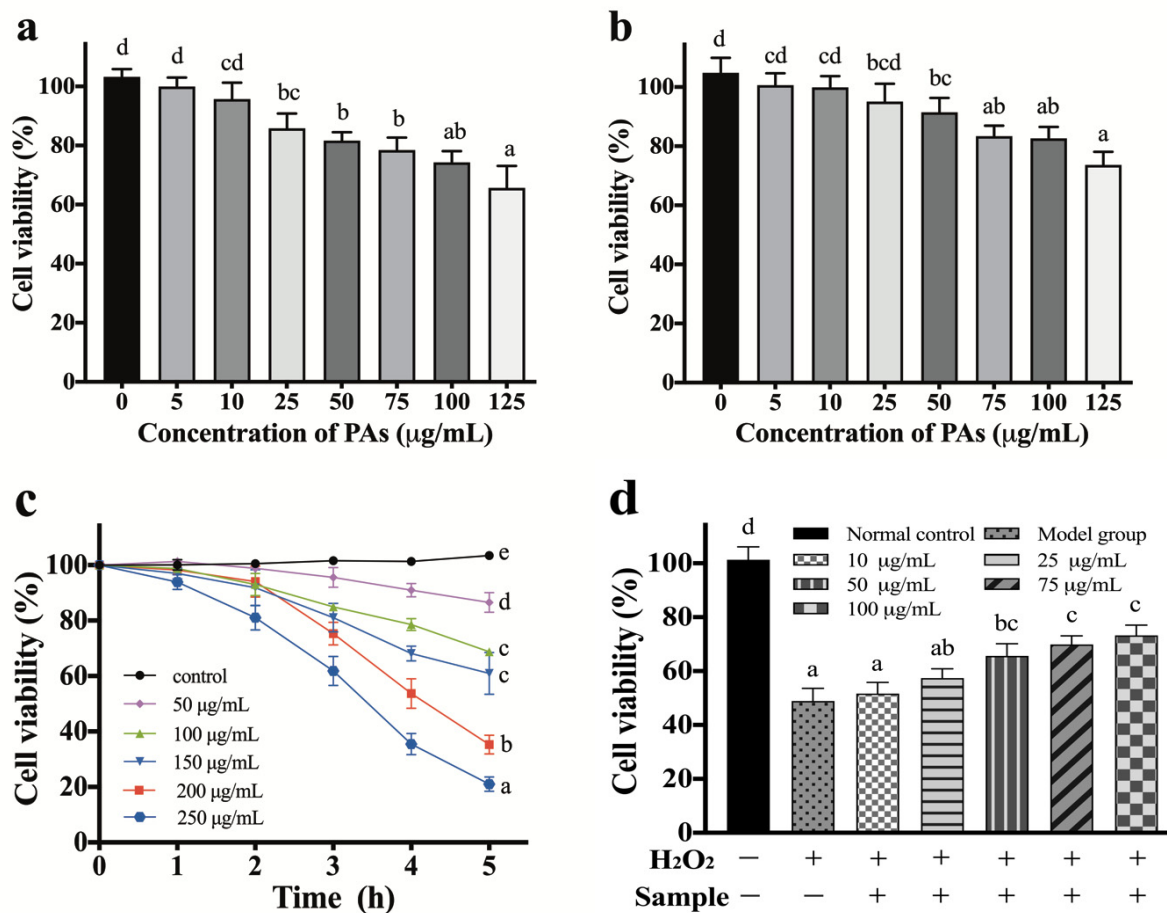


Figure 7. Cytotoxicity analysis of PKLPs by using various cells. (a) Caco-2 cells; (b) HepG-2 cells; (c) cell viability effect by various concentration of H_2O_2 (0–250 $\mu\text{g/mL}$); and (d) antioxidant potential of PKLPs on the H_2O_2 -induced Caco-2 cells model after 24 h of incubation. Mean \pm SD with different alphabet superscripts within the same column and analytical parameter indicate that values differ significantly ($p < 0.05$).

In addition, H_2O_2 is a typical member of the ROS family, which were widely used to construct the oxidative injury model to evaluate the natural extracted PA effect on anticancer cells [57]. As showed in Figure 7c, the cell viability decreased dramatically ($p < 0.05$) when exposed to the highest concentration of H_2O_2 (250 $\mu\text{g/mL}$) compared to the

low concentration of H₂O₂ (0–100 µg/mL). In particular, 53.69 ± 7.29% treated cells were viable after being treated with 100 µM of H₂O₂ for 4 h at 37 °C. As this value was close to the IC₅₀, this indicated that the H₂O₂-injured-Caco-2 model was established. Additionally, for the antioxidant assay, a moderate increase was found when Caco-2 cells were treated with appropriate concentrations of PAs (10–25 µg/mL) for 24 h before H₂O₂ treatment. Furthermore, a significant increase ($p < 0.05$) was happened when PKLP concentration increased to 100 µg/mL compared to 10 µg/mL (Figure 7d). The potential cellular redox activity might come from the increase in the reactivity of PAs with the oxidizing radicals that prevent the dissociation of both intramolecular and intermolecular disulfide bonds. This process is necessary for protein activity regulation that affects several cellular signal pathways and enzymatic reactions [58]. Additionally, the differences in PKLP cytotoxicity and cytoprotection were due to their dose dependent impact on the cellular pathways of the same cells [59], in which only at the lowest concentrations was a slight cytoprotection assayed. Meng et al. [60] reported that the cellular antioxidant activity is one of the best methods to explain the real redox homeostasis impact of natural phytochemicals that benefit human health.

4. Conclusions

In this study, the optimum US conditions on the extraction of bioactive and functional PAs were demonstrated. The four most important factors which affect the extraction of PAs and their potential interactions were evaluated to optimize their conditions. In conclusion, the characterization of PKLPs could be used as a functional food ingredient considering its potent antioxidant potential activity, which would have broad prospects and substantial economic benefits. The relationship between structure and bioactivity of PKLPs warrants further studies. This investigation is providing important information on the correlation between the potential impact of the extraction method on the formation and modifications of extracted PAs.

Supplementary Materials: The following are available online at <https://www.mdpi.com/article/10.3390/antiox10081317/s1>, Table S1. Extracted compositions identified peaks area by HPLC-QTOF-MS/MS.

Author Contributions: Conceptualization, J.-M.L. and J.-C.C.; methodology, J.-M.L.; software, J.-M.L. and Y.-Y.Z.; validation, J.-C.C. and M.G.; formal analysis, J.-M.L. and Y.-Y.Z.; investigation and Y.-Y.Z., J.-M.L.; resources, J.-C.C. and X.-Q.Y.; data curation, J.-M.L.; writing—original draft preparation, J.-M.L. and M.G.; writing—review and editing, M.G. and J.-M.L.; visualization, M.G. and J.-M.L.; supervision, J.-C.C.; project administration, J.-C.C. and X.-Q.Y.; funding acquisition, J.-C.C. and X.-Q.Y. All authors have read and agreed to the published version of the manuscript.

Funding: This research and its APC were funded by the National Key Research and Development Program of China (2017YFD0400704).

Institutional Review Board Statement: Not applicable.

Informed Consent Statement: Not applicable.

Acknowledgments: The authors would like to acknowledge Zhejiang University central labs and the National Key Research and Development Program of China for their support during the study investigations.

Conflicts of Interest: The authors declare no conflict of interest.

Abbreviations

| | |
|------------------|-----------------------------------|
| US | Using ultrasound |
| PA | Proanthocyanidins |
| PKLPs | Purified kiwi leaves Pas |
| S/S | Solvent to solid ration |
| UAE | Ultrasound-assisted extraction |
| ME | Maceration extraction |
| RSM | Response surface methodology |
| CCD | Central composite design |
| TPC | Total phenolics content |
| DW | Dry weight |
| PC | Procyanidin |
| DMEM | Dulbecc's modified Eagle medium |
| FBS | Foetal bovine serum |
| PBS | Phosphate-buffered solution |
| P/S | Penicillin/streptomycin |
| MTT | Methyl thiazolyl tetrazolium |
| WD | Weight basis |
| IC ₅₀ | The half-inhibitory concentration |

References

- Silva, A.M.; Pinto, D.; Fernandes, I.; Goncalves Albuquerque, T.; Costa, H.S.; Freitas, V.; Rodrigues, F.; Oliveira, M. Infusions and decoctions of dehydrated fruits of *actinidia arguta* and *actinidia deliciosa*: Bioactivity, radical scavenging activity and effects on cells viability. *Food Chem.* **2019**, *289*, 625–634. [[CrossRef](#)]
- Marangi, F.; Pinto, D.; de Francisco, L.; Alves, R.C.; Puga, H.; Sut, S.; Dall'Acqua, S.; Rodrigues, F.; Oliveira, M. Hardy kiwi leaves extracted by multi-frequency multimode modulated technology: A sustainable and promising by-product for industry. *Food Res. Int.* **2018**, *112*, 184–191. [[CrossRef](#)]
- Almeida, D.; Pinto, D.; Santos, J.; Vinha, A.F.; Palmeira, J.; Ferreira, H.N.; Rodrigues, F.; Oliveira, M. Hardy kiwifruit leaves (*actinidia arguta*): An extraordinary source of value-added compounds for food industry. *Food Chem.* **2018**, *259*, 113–121. [[CrossRef](#)]
- Gouda, M.; El-Din Bekhit, A.; Tang, Y.; Huang, Y.; Huang, L.; He, Y.; Li, X. Recent innovations of ultrasound green technology in herbal phytochemistry: A review. *Ultrason. Sonochem.* **2021**, *73*, 105538. [[CrossRef](#)]
- Unusan, N. Proanthocyanidins in grape seeds: An updated review of their health benefits and potential uses in the food industry. *J. Funct. Foods* **2020**, *67*, 103861. [[CrossRef](#)]
- Rauf, A.; Imran, M.; Abu-Izneid, T.; Iahtisham Ul, H.; Patel, S.; Pan, X.; Naz, S.; Sanches Silva, A.; Saeed, F.; Rasul Suleria, H.A. Proanthocyanidins: A comprehensive review. *Biomed. Pharmacother.* **2019**, *116*, 108999. [[CrossRef](#)] [[PubMed](#)]
- Tamura, T.; Ozawa, M.; Tanaka, N.; Arai, S.; Mura, K. Bacillus cereus response to a proanthocyanidin trimer, a transcriptional and functional analysis. *Curr. Microbiol.* **2016**, *73*, 115–123. [[CrossRef](#)]
- Ravindranathan, P.; Pasham, D.; Balaji, U.; Cardenas, J.; Gu, J.H.; Toden, S.; Goel, A. Mechanistic insights into anticancer properties of oligomeric proanthocyanidins from grape seeds in colorectal cancer. *Carcinogenesis* **2018**, *39*, 767–777. [[CrossRef](#)] [[PubMed](#)]
- Sun, Y.; Xiu, C.; Liu, W.; Tao, Y.; Wang, J.; Qu, Y.I. Grape seed proanthocyanidin extract protects the retina against early diabetic injury by activating the nrf2 pathway. *Exp. Ther. Med.* **2016**, *11*, 1253–1258. [[CrossRef](#)]
- Zheng, Y.; Tian, J.; Kong, X.; Wu, D.; Chen, S.; Liu, D.; Ye, X. Proanthocyanidins from chinese berry leaves modified the physicochemical properties and digestive characteristic of rice starch. *Food Chem.* **2021**, *335*, 127666. [[CrossRef](#)] [[PubMed](#)]
- Amoako, D.B.; Awika, J.M. Resistant starch formation through intrahelical v-complexes between polymeric proanthocyanidins and amylose. *Food Chem.* **2019**, *285*, 326–333. [[CrossRef](#)] [[PubMed](#)]
- Qin, Z.; Liu, H.-M.; Ma, Y.-X.; Wang, X.-D. Developments in extraction, purification, and structural elucidation of proanthocyanidins (2000–2019). *Stud. Nat. Prod. Chem.* **2021**, *68*, 347–391.
- Cao, J.; Chen, L.; Li, M.; Cao, F.; Zhao, L.; Su, E. Efficient extraction of proanthocyanidin from ginkgo biloba leaves employing rationally designed deep eutectic solvent-water mixture and evaluation of the antioxidant activity. *J. Pharmaceut. Biomed. Anal.* **2018**, *158*, 317–326. [[CrossRef](#)] [[PubMed](#)]
- Ran, L.; Yang, C.; Xu, M.; Yi, Z.; Ren, D.; Yi, L. Enhanced aqueous two-phase extraction of proanthocyanidins from grape seeds by using ionic liquids as adjuvants. *Sep. Purif. Technol.* **2019**, *226*, 154–161. [[CrossRef](#)]
- Jug, U.; Vovk, I.; Glavnik, V.; Makuc, D.; Naumoska, K. Off-line multidimensional high performance thin-layer chromatography for fractionation of japanese knotweed rhizome bark extract and isolation of flavan-3-ols, proanthocyanidins and anthraquinones. *J. Chromatogr. A* **2021**, *1637*, 461802. [[CrossRef](#)] [[PubMed](#)]
- Boulatov, R. The liberating force of ultrasound. *Nat. Chem.* **2021**, *13*, 112–114. [[CrossRef](#)]

17. Hu, B.; Li, C.; Qin, W.; Zhang, Z.; Liu, Y.; Zhang, Q.; Liu, A.; Jia, R.; Yin, Z.; Han, X.; et al. A method for extracting oil from tea (*Camellia sinensis*) seed by microwave in combination with ultrasonic and evaluation of its quality. *Ind. Crop. Prod.* **2019**, *131*, 234–242. [[CrossRef](#)]
18. Rashed, M.M.; Tong, Q.; Abdelhai, M.H.; Gasmalla, M.A.; Ndayishimiye, J.B.; Chen, L.; Ren, F. Effect of ultrasonic treatment on total phenolic extraction from *Lavandula pubescens* and its application in palm olein oil industry. *Ultrason. Sonochem.* **2016**, *29*, 39–47. [[CrossRef](#)]
19. Nutrizio, M.; Gajdos Kljusuric, J.; Marijanovic, Z.; Dubrovic, I.; Viskic, M.; Mikolaj, E.; Chemat, F.; Rezek Jambrak, A. The potential of high voltage discharges for green solvent extraction of bioactive compounds and aromas from rosemary (*rosmarinus officinalis* L.)—computational simulation and experimental methods. *Molecules* **2020**, *25*, 3711. [[CrossRef](#)]
20. Nguyen, T.M.C.; Gavahian, M.; Tsai, P.-J. Effects of ultrasound-assisted extraction (uae), high voltage electric field (hvef), high pressure processing (hpp), and combined methods (hvef+uae and hpp+uae) on gac leaves extraction. *LWT* **2021**, *143*, 111131. [[CrossRef](#)]
21. Xu, D.P.; Zheng, J.; Zhou, Y.; Li, Y.; Li, S.; Li, H.B. Ultrasound-assisted extraction of natural antioxidants from the flower of *limonium sinuatum*: Optimization and comparison with conventional methods. *Food Chem.* **2017**, *217*, 552–559. [[CrossRef](#)] [[PubMed](#)]
22. Hussein, L.; Gouda, M.; Buttar, H.S. Pomegranate, its components and modern deliverable formulations as potential botanicals in the prevention and treatment of various cancers. *Curr. Drug Deliv.* **2021**, *18*, 1–15. [[CrossRef](#)] [[PubMed](#)]
23. Ahmed, F.E.; Gouda, M.M.; Hussein, L.A.; Ahmed, N.C.; Vos, P.W.; Mohammad, M.A. Role of melt curve analysis in interpretation of nutrigenomics' microrna expression data. *Cancer Genom Proteom* **2017**, *14*, 469–481.
24. Shanmugam, M.K.; Lee, J.H.; Chai, E.Z.; Kanchi, M.M.; Kar, S.; Arfuso, F.; Dharmarajan, A.; Kumar, A.P.; Ramar, P.S.; Looi, C.Y.; et al. Cancer prevention and therapy through the modulation of transcription factors by bioactive natural compounds. *Semin. Cancer Biol.* **2016**, *40–41*, 35–47. [[CrossRef](#)] [[PubMed](#)]
25. Keum, N.; Giovannucci, E. Global burden of colorectal cancer: Emerging trends, risk factors and prevention strategies. *Nat. Rev. Gastroenterol. Hepatol.* **2019**, *16*, 713–732. [[CrossRef](#)]
26. Cilla, A.; Rodrigo, M.J.; Zacarias, L.; De Ancos, B.; Sanchez-Moreno, C.; Barbera, R.; Alegria, A. Protective effect of bioaccessible fractions of citrus fruit pulps against h2o2-induced oxidative stress in caco-2 cells. *Food Res. Int.* **2018**, *103*, 335–344. [[CrossRef](#)]
27. Martin-Garcia, B.; Pasini, F.; Verardo, V.; Diaz-de-Cerio, E.; Tylewicz, U.; Gomez-Caravaca, A.M.; Caboni, M.F. Optimization of sonotrode ultrasonic-assisted extraction of proanthocyanidins from brewers' spent grains. *Antioxidants* **2019**, *8*, 282. [[CrossRef](#)] [[PubMed](#)]
28. Xu, C.-C.; Wang, B.; Pu, Y.-Q.; Tao, J.-S.; Zhang, T. Advances in extraction and analysis of phenolic compounds from plant materials. *Chin. J. Nat. Med.* **2017**, *15*, 721–731. [[CrossRef](#)]
29. Luo, X.; Cui, J.; Zhang, H.; Duan, Y.; Zhang, D.; Cai, M.; Chen, G. Ultrasound assisted extraction of polyphenolic compounds from red sorghum (*sorghum bicolor* L.) bran and their biological activities and polyphenolic compositions. *Ind. Crop. Prod.* **2018**, *112*, 296–304. [[CrossRef](#)]
30. Das, A.K.; Dewanjee, S. Optimization of extraction using mathematical models and computation. In *Computational Phytochemistry*; Elsevier: Amsterdam, The Netherlands, 2018; pp. 75–106.
31. Jovanović, A.A.; Đorđević, V.B.; Zdunić, G.M.; Pljevljakušić, D.S.; Šavikin, K.P.; Gođevac, D.M.; Bugarski, B.M. Optimization of the extraction process of polyphenols from thymus serpyllum L. Herb using maceration, heat- and ultrasound-assisted techniques. *Sep. Purif. Technol.* **2017**, *179*, 369–380. [[CrossRef](#)]
32. Gouda, M.; Chen, K.; Li, X.; Liu, Y.; He, Y. Detection of microalgae single-cell antioxidant and electrochemical potentials by gold microelectrode and raman micro-spectroscopy combined with chemometrics. *Sens. Actuators B Chem.* **2021**, *329*, 129229. [[CrossRef](#)]
33. Huang, H.; Belwal, T.; Jiang, L.; Hu, J.; Limwachiranon, J.; Li, L.; Ren, G.; Zhang, X.; Luo, Z. Valorization of lotus byproduct (receptaculum nelumbinis) under green extraction condition. *Food Bioprod. Process.* **2019**, *115*, 110–117. [[CrossRef](#)]
34. Gao, X.; Xu, D.; Zhang, X.; Zhao, H. Protective effect of lemon peel polyphenols on oxidative stress-induced damage to human keratinocyte hacat cells through activation of the nrf2/ho-1 signaling pathway. *Front. Nutr.* **2020**, *7*, 606776. [[CrossRef](#)] [[PubMed](#)]
35. Liang, R.; Cheng, S.; Dong, Y.; Ju, H. Intracellular antioxidant activity and apoptosis inhibition capacity of pef-treated kdch in hepg2 cells. *Food Res. Int.* **2019**, *121*, 336–347. [[CrossRef](#)]
36. Bellumori, M.; Innocenti, M.; Binello, A.; Boffa, L.; Mulinacci, N.; Cravotto, G. Selective recovery of rosmarinic and carnosic acids from rosemary leaves under ultrasound- and microwave-assisted extraction procedures. *Comptes Rendus Chim.* **2016**, *19*, 699–706. [[CrossRef](#)]
37. Cravotto, G.; Gaudino, E.C.; Cintas, P. On the mechanochemical activation by ultrasound. *Chem. Soc. Rev.* **2013**, *42*, 7521–7534. [[CrossRef](#)] [[PubMed](#)]
38. Duan, H.-Y.; Wang, Y.-X.; Wang, L.-J.; Min, Y.-Q.; Zhang, X.-H.; Du, B.-Y. An investigation of the selective chain scission at centered diels–alder mechanophore under ultrasonication. *Macromolecules* **2017**, *50*, 1353–1361. [[CrossRef](#)]
39. Zhao, L.; Zhao, G.; Chen, F.; Wang, Z.; Wu, J.; Hu, X. Different effects of microwave and ultrasound on the stability of (all-e)-astaxanthin. *J. Agric. Food Chem.* **2006**, *54*, 8346–8351. [[CrossRef](#)] [[PubMed](#)]
40. Patil, D.M.; Akamanchi, K.G. Ultrasound-assisted rapid extraction and kinetic modelling of influential factors: Extraction of camptothecin from *Nothapodytes nimmoniana* plant. *Ultrason. Sonochem.* **2017**, *37*, 582–591. [[CrossRef](#)]

41. Huo, S.; Zhao, P.; Shi, Z.; Zou, M.; Yang, X.; Warszawik, E.; Loznik, M.; Gostl, R.; Herrmann, A. Mechanochemical bond scission for the activation of drugs. *Nat. Chem.* **2021**, *13*, 131–139. [[CrossRef](#)]
42. Yang, T.; Fang, L.; Lin, T.; Li, J.; Zhang, Y.; Zhou, A.; Xie, J. Ultrasonicated sour jujube seed flavonoids extract exerts ameliorative antioxidant capacity and reduces abeta-induced toxicity in caenorhabditis elegans. *J. Ethnopharmacol.* **2019**, *239*, 111886. [[CrossRef](#)] [[PubMed](#)]
43. Wang, Y.; Zhang, X.; Ma, X.; Zhang, K.; Li, S.; Wang, X.; Liu, X.; Liu, J.; Fan, W.; Li, Y.; et al. Study on the kinetic model, thermodynamic and physicochemical properties of glycyrrhiza polysaccharide by ultrasonic assisted extraction. *Ultrason. Sonochem.* **2019**, *51*, 249–257. [[CrossRef](#)] [[PubMed](#)]
44. Skotti, E.; Anastasaki, E.; Kanellou, G.; Polissiou, M.; Tarantilis, P.A. Total phenolic content, antioxidant activity and toxicity of aqueous extracts from selected greek medicinal and aromatic plants. *Ind. Crop. Prod.* **2014**, *53*, 46–54. [[CrossRef](#)]
45. Alenyorege, E.A.; Ma, H.; Aheto, J.H.; Ayim, I.; Chikari, F.; Osa, R.; Zhou, C. Response surface methodology centred optimization of mono-frequency ultrasound reduction of bacteria in fresh-cut chinese cabbage and its effect on quality. *LWT* **2020**, *122*, 108991. [[CrossRef](#)]
46. Tchabo, W.; Ma, Y.; Engmann, F.N.; Zhang, H. Ultrasound-assisted enzymatic extraction (uaee) of phytochemical compounds from mulberry (*morus nigra*) must and optimization study using response surface methodology. *Ind. Crop. Prod.* **2015**, *63*, 214–225. [[CrossRef](#)]
47. Leontowicz, H.; Leontowicz, M.; Latocha, P.; Jesion, I.; Park, Y.S.; Katrich, E.; Barasch, D.; Nemirovski, A.; Gorinstein, S. Bioactivity and nutritional properties of hardy kiwi fruit *actinidia arguta* in comparison with *actinidia deliciosa* ‘hayward’ and *actinidia eriantha* ‘bidan’. *Food Chem.* **2016**, *196*, 281–291. [[CrossRef](#)] [[PubMed](#)]
48. Esua, O.J.; Cheng, J.H.; Sun, D.W. Optimisation of treatment conditions for reducing *shewanella putrefaciens* and *salmonella typhimurium* on grass carp treated by thermoultrasound-assisted plasma functionalized buffer. *Ultrason. Sonochem.* **2021**, *76*, 105609. [[CrossRef](#)] [[PubMed](#)]
49. Ismail, B.B.; Guo, M.; Pu, Y.; Wang, W.; Ye, X.; Liu, D. Valorisation of baobab (*adansonia digitata*) seeds by ultrasound assisted extraction of polyphenolics. Optimisation and comparison with conventional methods. *Ultrason. Sonochem.* **2019**, *52*, 257–267. [[CrossRef](#)]
50. Allahyari, A.; Masoum, S.; Akhbari, M.; Hamedi, S.; Mazoochi, A. Experimental design approach in optimization of some effective variables on quantity and quality extraction of essential oil from *rosa damascena* mill. *J. Iran. Chem. Soc.* **2021**, *18*, 2437–2445. [[CrossRef](#)]
51. Kumari, M.; Gupta, S.K. Response surface methodological (rsm) approach for optimizing the removal of trihalomethanes (thms) and its precursor’s by surfactant modified magnetic nanoadsorbents (smnp)—An endeavor to diminish probable cancer risk. *Sci. Rep.* **2019**, *9*, 18339. [[CrossRef](#)]
52. Guo, N.; Zou, Y.-P.; Li, H.-K.; Kou, P.; Liu, Z.-M.; Fu, Y.-J. Effective extraction and recovery of linarin from *chrysanthemum indicum* l. Flower using deep eutectic solvents. *Microchem. J.* **2020**, *159*, 105586. [[CrossRef](#)]
53. Deng, J.; Xu, Z.; Xiang, C.; Liu, J.; Zhou, L.; Li, T.; Yang, Z.; Ding, C. Comparative evaluation of maceration and ultrasonic-assisted extraction of phenolic compounds from fresh olives. *Ultrason. Sonochem.* **2017**, *37*, 328–334. [[CrossRef](#)] [[PubMed](#)]
54. Fourie, E.; Aleixandre-Tudo, J.L.; Mihnea, M.; du Toit, W. Partial least squares calibrations and batch statistical process control to monitor phenolic extraction in red wine fermentations under different maceration conditions. *Food Control* **2020**, *115*, 107303. [[CrossRef](#)]
55. Pudziuvelyte, L.; Jakštas, V.; Ivanauskas, L.; Laukevičienė, A.; Ibe, C.F.D.; Kursvietiene, L.; Bernatoniene, J. Different extraction methods for phenolic and volatile compounds recovery from *elsholtzia ciliata* fresh and dried herbal materials. *Ind. Crop. Prod.* **2018**, *120*, 286–294. [[CrossRef](#)]
56. Magdaleno-Tapia, C.; Quifer-Rada, P.; Rodriguez-Rodriguez, E.; Estevez-Santiago, R.; Waterhouse, A.L.; Lamuela-Reventos, R.M.; Olmedilla-Alonso, B.; Perez-Jimenez, J. Evaluation of the potential of total proanthocyanidin content in feces as an intake biomarker. *Food Res. Int.* **2021**, *145*, 110390. [[CrossRef](#)]
57. Jung, H.; Lee, H.J.; Cho, H.; Lee, K.; Kwak, H.-K.; Hwang, K.T. Anthocyanins in *rubus* fruits and antioxidant and anti-inflammatory activities in raw 264.7 cells. *Food Sci. Biotechnol.* **2015**, *24*, 1879–1886. [[CrossRef](#)]
58. Matsuzawa, A. Thioredoxin and redox signaling: Roles of the thioredoxin system in control of cell fate. *Arch. Biochem. Biophys.* **2017**, *617*, 101–105. [[CrossRef](#)]
59. Juan-Garcia, A.; Montesano, D.; Manes, J.; Juan, C. Cytoprotective effects of carotenoids-rich extract from *lycium barbarum* l. On the beauvericin-induced cytotoxicity on caco-2 cells. *Food Chem. Toxicol. Int. J. Publ. Br. Ind. Biol. Res. Assoc.* **2019**, *133*, 110798. [[CrossRef](#)]
60. Meng, D.; Zhang, P.; Zhang, L.; Wang, H.; Ho, C.-T.; Li, S.; Shahidi, F.; Zhao, H. Detection of cellular redox reactions and antioxidant activity assays. *J. Funct. Foods* **2017**, *37*, 467–479. [[CrossRef](#)]